J Solid State Electrochem (2009) 13:1687–1694
DOI 10.1007/s10008-008-0642-z

ORIGINAL PAPER

Impact of sensitization on dissolution process of AISI 304 stainless steel during intergranular corrosion evaluated using DEIS technique

A. Arutunow · K. Darowicki

Received: 9 May 2008 / Revised: 28 July 2008 / Accepted: 30 July 2008 / Published online: 22 August 2008

Abstract The paper presents the results of instantaneous impedance changes measurements vs. reactivation potential performed by means of dynamic electrochemical impedance spectroscopy (DEIS) technique for AISI 304 stainless steel (SS) dissolution process during intergranular corrosion (IG) in 0.5 M H_2SO_4+0.01 M KSCN solution. With the use of DEIS method, it was possible to estimate dynamic changes of the examined system's impedance in conditions of proceeding IG process. Furthermore, the paper proposes an alternative way of evaluating AISI 304 stainless steel dissolution rate during intergranular corrosion based on approximation to theory of iron dissolution in sulfuric acid medium. Simultaneously, based on the DEIS measurements, information about the degree of sensitization of the examined material were obtained. Performed research revealed the advantages of the DEIS technique over the classical double-loop electrochemical potentiokinetic reactivation tests when investigating intergranular corrosion process.

Keywords Dissolution process · Intergranular corrosion · DEIS · AISI 304 stainless steel

Introduction

Austenitic stainless steels (SS)—containing 18% chromium and 8% nickel—are engineering materials widely used in many branches of industry due to their good mechanical properties and corrosion resistance at elevated temperatures. However, the precipitation of intermetallic compounds at grain boundaries affects this resistance [1–3]. Exposure to high temperatures ranging from 500 to 800 °C, during welding or service, leads to precipitation of chromium rich carbides (type $Cr_{23}C_6$) or sigma phase (Fe-Cr-Mo) at grain boundaries and formation of chromium depletion regions adjacent to these carbides. Therefore, stainless steels with less than 12–13 wt.% of chromium- and chromium-depleted regions at grain boundaries are known to have undergone sensitization [1–5].

Intergranular corrosion of austenitic stainless steels is explained by the chromium depletion theory [6, 7], which shows that the extent of chromium-depleted zones at grain boundaries indicates directly the material's susceptibility to IG process and in the presence of residual stresses and strain to IGSCC as well in the final stage [8].

According to the ASTM standard, metallographic etching and weight-loss tests are regularly performed to assess degree of sensitization (DOS) of austenitic stainless steels [7–15]. The disadvantages of these evaluation techniques are the considerable consumption of etchant and long testing period. Since anodic dissolution of austenitic SS in an electrolyte is an electrochemical process, estimating DOS of austenitic stainless steels should be possible by means of electrochemical methods. Many electrochemical methods were proposed to determine DOS of stainless steels in the literature [16, 17]. Among them, anodic polarization tests [18] were the most commonly used approaches.

The search for a rapid, quantitative, and non-destructive test method has lead many researchers to develop double-loop electrochemical potentiokinetic reactivation (DL-EPR) tests [2, 3, 19–25]. This technique was especially applied in

Presented at the international conference CORROSION TODAY held in Gdansk-Sobieszewo, Poland, 23 to 26 April 2008.

A. Arutunow (✉) · K. Darowicki
Department of Electrochemistry,
Corrosion and Materials Engineering,
Gdansk University of Technology,
G. Narutowicza 11/12, 80-952 Gdansk, Poland
e-mail: anka@chem.pg.gda.pl

detecting DOS of AISI 304 stainless steels. Nevertheless, it is worth to emphasize certain disadvantages of this method, among the most important of which are high-amplitude perturbation signal, determination of DOS only, and finally, lack of information related to the mechanism and rate of IG.

Classical electrochemical impedance spectroscopy (EIS) also provides information concerning the IG\ but only before and after the corrosion process, when the investigated system is in a stable state. Therefore, EIS cannot provide detailed characteristic of the proceeding corrosion processes. Nevertheless, AC impedance for the evaluation of DOS has not been reported yet. What is more important is that any information concerning the impedance assessment of the effective surface area of AISI 304 stainless steel dissolution process during intergranular corrosion cannot be found in the literature.

Such possibility can be achieved by using dynamic electrochemical impedance spectroscopy (DEIS). Due to its joint time–frequency procedure [26–30], DEIS allows to investigate the proceeding corrosion process in time and therefore obtain very detailed characteristic of the examined system. So far, DEIS was successfully applied in the examination of pitting corrosion [31–33], organic coatings [34], passive layer cracking process on austenitic stainless steels, and aluminum alloys [35–39], and in the investigation of the mechanism and kinetics of pickling of high-temperature oxidized 304 SS in HF-H_2SO_4 [40].

The objective of this paper is to evaluate dynamic changes of impedance of AISI 304 stainless steel dissolution process in conditions of proceeding intergranular corrosion by means of DEIS technique.

Experimental

Chemical composition of austenitic stainless steel used in this study is given in Table 1. Examined specimens were prepared according to instructions provided by the ASTM G108-94 standard [41]. The specimens were sensitized at 675 °C for 24 or 36 h. Corrosion potential of all sensitized specimens in the examined electrolyte solution was about E_{CORR}=−0.900 $V_{Hg,Hg2SO4|H2SO4}$ independently of the sensitization time. Non-sensitized (reference) specimens were also examined in order to make adequate comparison. The corrosion potentials of non-sensitized and sensitized specimens were the same. Thirty specimens of each type were investigated. The exposed area for all examined specimens was 0.5 cm^2.

DEIS measurements were performed in a three-electrode cell, in which mercury/mercury sulfate [Hg, Hg_2SO_4|$H_2SO_{4(0.5\ mol/dm3)}$] electrode was used as a reference electrode, and the auxiliary electrode was made of platinum net. The employed reference electrode is not in accordance with the ASTM G 108-94 standard, where saturated calomel electrode with controlled leakage rate is recommended. Instead, an electrode with electrolytic bridge filled with sulfuric acid was used. The concentration of the acid was the same as in the investigated electrolyte solution. This way, it was possible to avoid the risk of pitting corrosion due to the presence of chloride ions, which might have been transported to the solution from the electrolytic bridge filled with potassium chloride. The experiments were realized in 0.5 M $H_2SO_4^{-2}$+0.01 M KSCN solution.

DEIS measurements, in accordance with the measurement procedure given by the ASTM G108-94 standard [41] to guarantee conditions equivalent to the DL-EPR tests performed on AISI 304 stainless steel, were carried out "on-line," while the samples were polarized in temperature of electrolyte 30 °C±1: polarization from E_{CORR}= −0.900 $V_{Hg,Hg2SO4|H2SO4}$ to E=−0.200 $V_{Hg,Hg2SO4|H2SO4}$ (maintained for 2 min in the passive state), activation scan; and back to corrosion potential E_{CORR}=−0.900 $V_{Hg,Hg2SO4|H2SO4}$, reactivation scan.

The measurement setup was composed of a high-frequency potentiostat and a National Instruments PCI 6120 card, which generated the perturbation signal, as well as registered voltage perturbation and current response signals. Impedance measurements were executed for the frequency range 20 kHz–7 Hz. The average number of points per decade in the DEIS measurements was 5.

The choice of sampling frequency of 100 kHz resulted from the disposable measurement card settings. Proper selection of the sampling frequency in the DEIS measurements enables to reflect the highest measurement frequencies with very good precision. A multi-sinusoidal perturbation signal composed of 20 sinusoids was used for the measurements. The amplitudes of the perturbation signal were diversified within the range from 5 to 28 mV in order to measure DC current with acceptable accuracy using only one resistor for both low and high frequencies. In the case of low frequencies, higher amplitudes of the perturbation signal were applied, as opposed to the high frequency range in which lower amplitudes were selected.

Table 1 Normalized chemical composition of AISI 304 (average values)

C	Mn	Si	P	S	Cr	Ni	Fe
≤0.08%	≤2.0%	≤1.0%	≤0.045%	≤0.03%	18–20%	8–10.5%	Bal.

Background and more detailed description of the DEIS technique can be found in papers written by Darowicki and co-workers [26–28].

Results and discussion

Dependencies between DC current and potential, both in the activation and reactivation range, were obtained on the basis of proper filtering procedure, which is strictly connected with the DEIS technique [26–28]. As is presented in Eq. 1, both voltage perturbation and current response signals are composed of a DC term and the other one that describes impedance of the examined process. Thus, after filtering out the DC components from the perturbation and response signals, one obtains the relation i_{DC}= f(u_{DC}), equivalent to the classical polarization curve.

$$u_{DC} + \sum_{i=1}^{n} u_i \exp[-j(\omega_i t + \Psi_i)] \quad \rightarrow \quad \text{perturbation signal} \tag{1}$$

$$i_{DC} + \sum_{i=1}^{n} i_i \exp[-j(\omega_i t + \Psi_i + \Phi_i)] \quad \text{response signal}$$

where u_i and i_i are the signal amplitudes for the ith frequency, t is time, Ψ_i is the phase shift of perturbation/response signal, and Φ_i corresponds to the phase shift resulting from the character of the investigated process.

Accordingly, Figs. 1a–c depict DC current dependencies vs. activation and reactivation potentials recorded for the non-sensitized (reference) and sensitized specimens. Significant activation peaks can be observed for all investigated specimens, whereas the reactivation peaks can only be found for the sensitized specimens independently of the sensitization time. Analogical results would have been obtained by means of the classical DL-EPR technique.

However, with the use of DL-EPR tests, one can only obtain the ratio between maximal values of reactivation and activation current [i_{max}(reactivation)/i_{max}(activation)] defined as the DOS. Adequate results are gathered in Table 2. Hence, based on the DL-EPR measurements, it is difficult to determine the mechanism and rate of both AISI 304 stainless steel dissolution process and IG in the reactivation potential range. The values of DOS calculated for the reference specimens were all low, below 0.1, which implies their resistance to IG. On the contrary, specimens sensitized for 24 h and the ones sensitized for 36 h could be recognized as susceptible to IG because of DOS values exceeding 0.5. This is in good agreement with the instructions provided by the ASTM G108-94 standard [41].

Application of the DEIS method made it possible to record sets of instantaneous impedance spectra reflecting dynamic changes of the investigated system's impedance as a function of potential. Regarding the fact that the difference in dependencies between DC current and potential was only detected in the reactivation scans, Fig. 2a–c presents exemplary DEIS spectra recorded for the reference

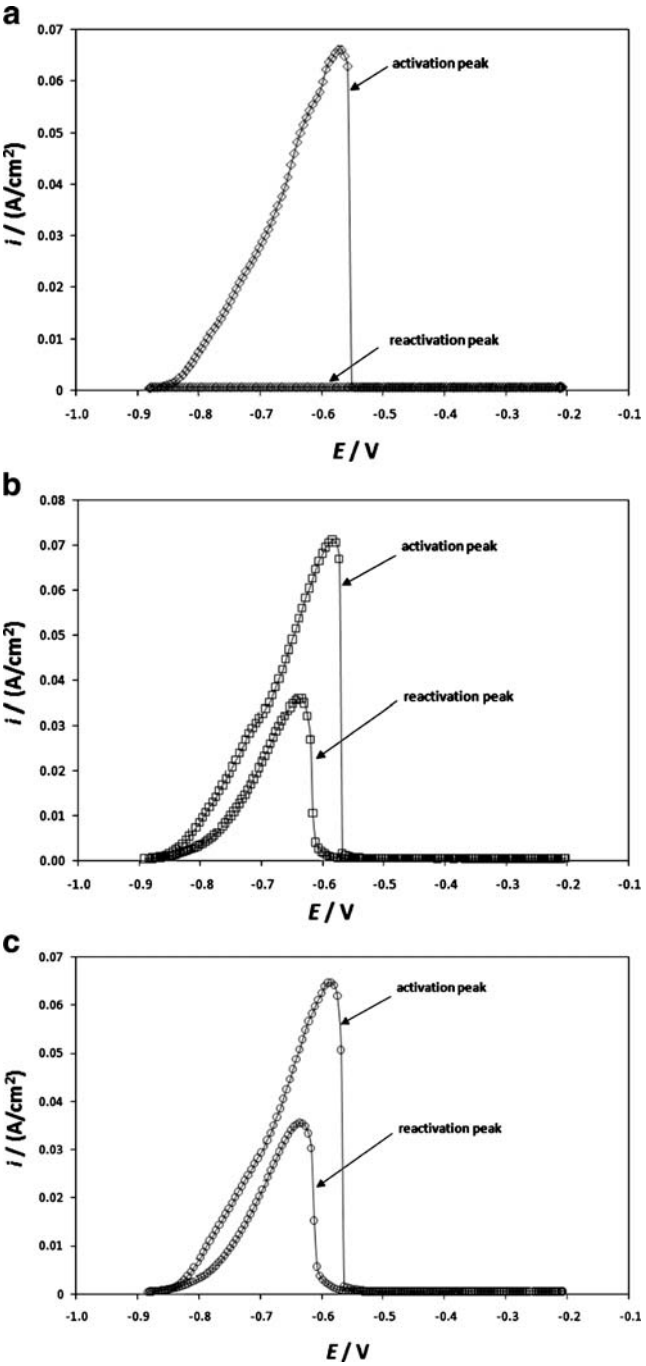

Fig. 1 Exemplary DC current changes vs. activation and reactivation potential obtained by filtering out the DC component from the voltage perturbation and current response signals recorded during the DEIS measurements in 0.5 M $H_2SO_4^{-2}$+0.01 M KSCN solution: **a** reference (non-sensitized) specimen, **b** specimen after 24 h of sensitization in 675 °C, **c** specimen after 36 h of sensitization in 675 °C

Table 2 Calculated values of the degree of sensitization (DOS) for the reference electrode and for the specimens of different sensitization time

Sample	i_{max}(reactivation)/ i_{max}(activation)
R (0.5 M H_2SO_4+0.01 M KSCN)	0.008
24 (0.5 M H_2SO_4+0.01 M KSCN)	0.503
36 (0.5 M H_2SO_4+0.01 M KSCN)	0.548

specimen and for the sensitized ones vs. reactivation potential (i.e., from about −0.550 V to about −0.870 V). Instantaneous impedance changes of the sensitized specimens were recorded as opposed to the reference ones. The impedance spectra of non-sensitized specimens exhibited capacitance character (passive state), indicating that no AISI 304 stainless steel dissolution process was detected, while the sensitized ones exhibited significant active–passive transition unequivocally involved with proceeding corrosion process.

Unquestionable is the shape of DEIS spectra that were recorded for the sensitized specimens and distribution of the measurement frequencies. Both correspond to the ones obtained for pure iron dissolution in sulfuric acid medium [42–45] and exhibit one inductance loop responsible for the presence of intermediate on the surface of examined specimens. Considering chemical composition of the investigated material and the theory presented by Armstrong et al. [44] and Epelboin et al. [45], it can be stated that, in the case of AISI 304 SS dissolution in conditions of IG, the most probable intermediate among other ones that could also be present is $Fe(OH)_{ads}$. Such a situation has been depicted in detail in Fig. 3, which illustrates exemplary 2D impedance spectra extracted from the reactivation potential range (from E=−0.705 V to E=−0.749 V) of the DEIS spectrogram that was recorded for the specimen sensitized for 36 h. Results presented in this form distinctly show activation character of registered impedance spectra and exclude the occurrence of diffusion process.

Intergranular corrosion is considered as one of the most difficult corrosion processes to predict due to its complicated mechanism. Taking into account the shape of registered DEIS spectra and the theory proposed by Armstrong et al. [44] and Epelboin et al. [45], the authors assumed that following reactions 2 and 3 could represent the mechanism of dissolution of AISI 304 stainless steel in conditions of proceeding intergranular corrosion:

$$Fe + OH^- \underset{k_{-2}}{\overset{k_2}{\rightleftarrows}} (FeOH)_{ads} + e \quad (2)$$

$$(FeOH)_{ads} \xrightarrow{k_3} Fe(OH)^+ + e \quad (3)$$

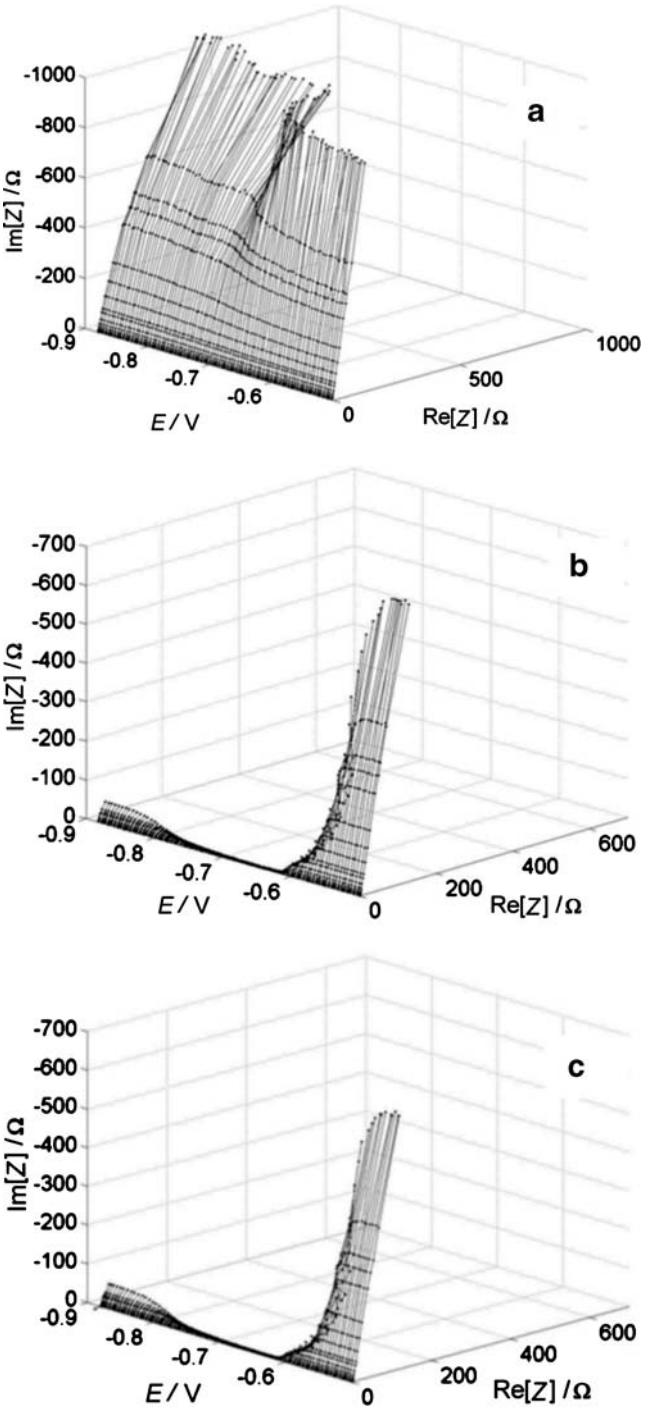

Fig. 2 Exemplary DEIS impedance spectra as a function of reactivation potential registered for AISI 304SS dissolution process during proceeding IG: **a** reference (non-sensitized) specimen, **b** specimen sensitized for 24 h in 675 °C, **c** specimen sensitized for 36 h in 675 °C

This kind of assumption can provide additional information about general character of IG process.

Analysis of recorded DEIS impedance spectra had to be performed to give detailed impedance characterization of AISI 304 stainless steel dissolution process in conditions of

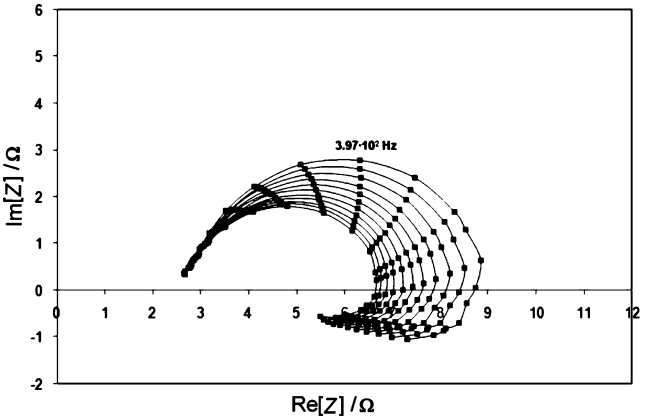

Fig. 3 2D impedance spectra extracted from the DEIS spectrogram, which was recorded as a function of reactivation potential (from E=−0.705 V to E=−0.749 V) for the sample sensitized for 36 h in 675 °C during the exposure to 0.5 M H_2SO_4+0.01 M KSCN solution

intergranular corrosion. The obtained results were analyzed by using equivalent circuit presented in Fig. 4. This equivalent circuit was successfully employed by Epelboin et al. [43] during studies over the AC impedance of iron dissolution in sulfuric acid medium. Fitting of the proper equivalent circuit was performed using professional ZSimpWin software. At this point, it should be emphasized that intergranular corrosion process occurs as a result of active–passive cell operation. Accordingly, $R_e(Q_pR_p)$ part of the circuit describes the passive state (chromium enriched) and was used to analyze impedance of the reference samples in reactivation range, while $R_e(C_{dl}(R_{ads}L)R_{ct})$ refers to the active state and determines grain boundaries impedance (chromium depletion zones directly related to the IG process) that was analyzed for the sensitized specimens. During the IG process, the surface of steel was not in the passive state; thus, impedance of the upper branch was very high and impedance of the lower one was very low (current flows along the path of the lowest resistance). The two branches of the equivalent circuit are connected in parallel. Since reciprocal of the upper branch impedance is very low, it can be omitted, and thus, the parameters of the upper branch (Q_p and R_p) can be neglected in analysis of the sensitized specimens.

Particular elements of equivalent circuit employed for the analysis of grain boundaries impedance in the reactivation range are described in Figs. 5, 6, 7, and 8. In general, dependencies of equivalent circuit parameters presented for the non-sensitized specimens as a function of reactivation potential describe surface state of the examined stainless steel. The dependencies for the sensitized specimens refer to the grain/grain boundary interface.

In Fig. 5, dynamic changes of the electrical double-layer capacitance vs. reactivation potential received for the non-sensitized and sensitized specimens are plotted. Slight decrease in the electrical double-layer capacitance with reactivation potential can be observed for the reference specimen, indicating stable passive state of the examined reference specimen in the reactivation potential range. This corresponds to the impedance spectra presented in Fig. 2a. It can be explained by the fact that the non-sensitized specimens did not exhibit susceptibility to intergranular corrosion resulted from the precipitation of $Cr_{23}C_6$ at grain boundaries and simultaneous formation of chromium depletion zones near the grain boundaries area. As a result, initiation of AISI 304 SS dissolution process was not possible. On the other hand, sensitized specimens revealed increase of about one order of magnitude in the electrical double-layer capacitance with reactivation potential independently of the sensitization time. Such a significant increase in the electrical double layer capacitance results from a decay of passivity at and near grain boundaries due to precipitation of $Cr_{23}C_6$ and simultaneous formation of chromium depletion zones. This enabled initiation of AISI 304 SS dissolution process, and its further intensification as the potential was changing in the cathodic direction.

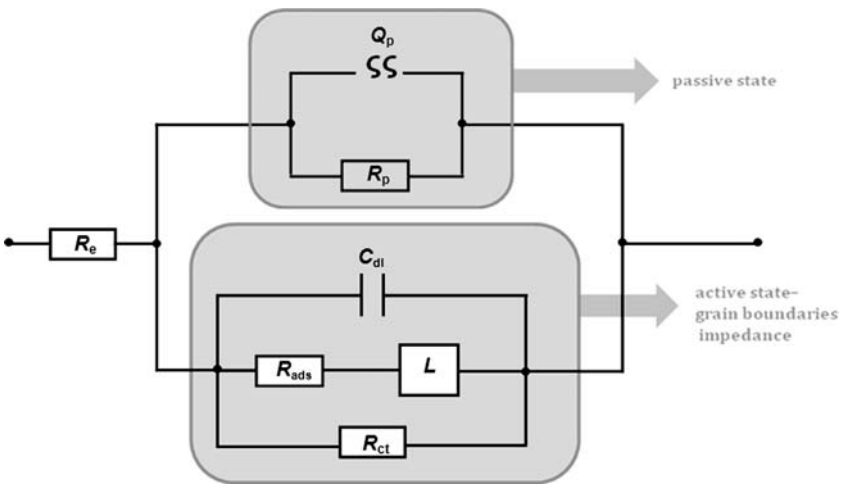

Fig. 4 Equivalent circuit applied to the analysis of IG process proceeding on AISI 304 stainless steel, where: R_e—the electrolyte resistance, Q_p—constant phase element, R_p—the passive layer resistance, C_{dl}—the electrical double layer capacitance, R_{ads}—the intermediate adsorption resistance, L—the inductance, R_{ct}—the charge transfer resistance

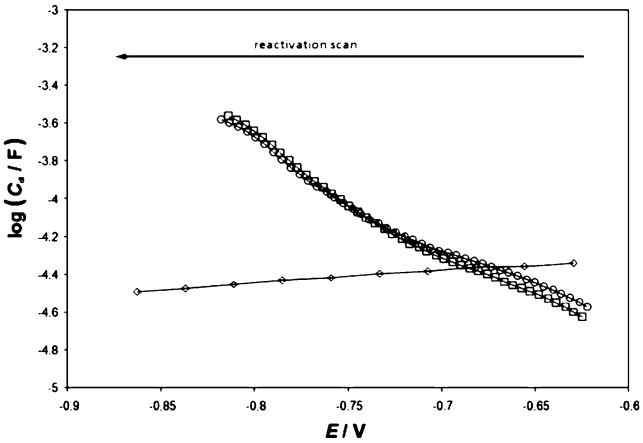

Fig. 5 Changes of the electrical double-layer capacitance as a function of reactivation potential obtained for the specimens made of AISI 304 stainless steel on the basis of the DEIS measurements in 0.5 M H_2SO_4+0.01 M KSCN solution: *diamond* reference (non-sensitized) specimen, *square* specimen sensitized for 24 h in 675 °C, *circle* specimen sensitized for 36 h in 675 °C

Moreover, when taking into consideration the electrochemical fundamentals of interfaces, which particularly includes the characterization of the electrical double layer, its capacitance can be described by the following Eq. 4 [46]:

$$C_{\mathrm{dl}} = \left(\frac{\partial q}{\partial E}\right) \tag{4}$$

where q=charge, E=potential.

Accordingly, the electrical double layer capacitance is directly proportional to the charge and inversely proportional to the potential. That explains the increase of the electrical double-layer capacitance due to simultaneously proceeding cathodic polarization and AISI 304 SS dissolution process resulting in Fe^{2+} formation.

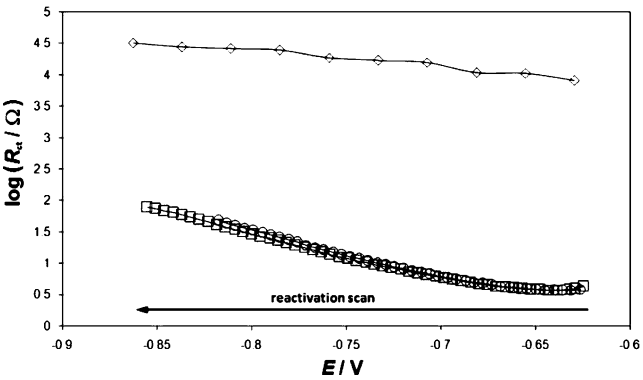

Fig. 6 Changes of the charge transfer resistance vs. reactivation potential obtained for the specimens made of AISI 304 stainless steel on the basis of the DEIS measurements in 0.5 M H_2SO_4+0.01 M KSCN solution: *diamond* reference (non-sensitized) specimen, *square* specimen sensitized for 24 h in 675 °, *circle* specimen sensitized for 36 h in 675 °C

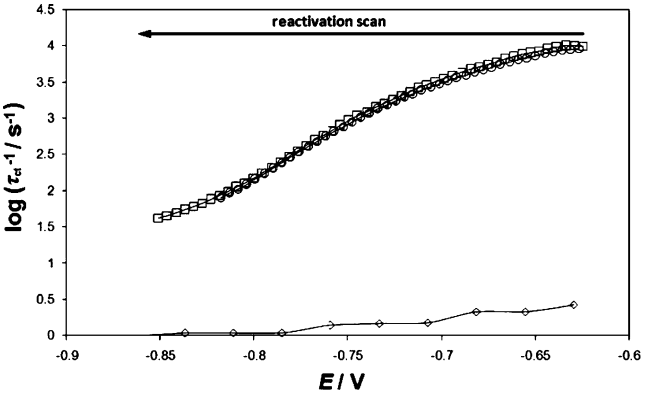

Fig. 7 Changes of the rate of charge transfer reaction as a function of reactivation potential obtained for the specimens made of AISI 304 stainless steel on the basis of the DEIS measurements in 0.5 M H_2SO_4+ 0.01 M KSCN solution: *diamond* reference (non-sensitized) specimen, *square* specimen sensitized for 24 h in 675 °C, *circle* specimen sensitized for 36 hours in 675 °C

Changes of the charge transfer resistance with decreasing reactivation potential are presented in Fig. 6. For non-sensitized specimen, instantaneous changes of the charge transfer resistance are about two orders of magnitude higher than for the sensitized specimens, which confirms proceeding corrosion processes. In the reactivation potential range, the charge transfer resistance increases by one order of magnitude with potential increase to the cathodic direction independently of the sensitization time. Increase in the charge transfer resistance detected with increasing cathodic polarization results from the intermediate adsorption on the electrode's surface due to proceeding dissolution process.

At this point, it is important to emphasize that both above-described parameters, that is C_{dl} and R_{ct}, depend on the parameter of attacked grain boundaries area and cannot be directly used to evaluate rate of AISI 304 stainless steel dissolution process. In order to eliminate this problem, values of these parameters were multiplied giving the

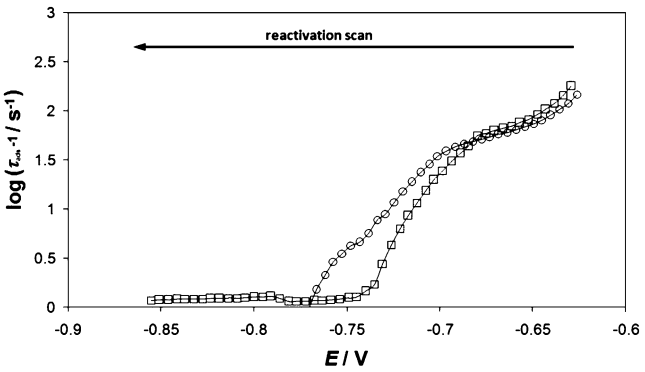

Fig. 8 Changes of the rate of intermediate adsorption process versus reactivation potential obtained for the specimens made of AISI 304 stainless steel on the basis of the DEIS measurements in 0.5 M H_2SO_4+ 0.01 M KSCN solution: *square* specimen sensitized for 24 h in 675 °, *circle* specimen sensitized for 36 h in 675 °C

product $R_{ct}{\cdot}C_{dl}$ equivalent with the time-constant of the charge transfer reaction. Furthermore, having taken a reciprocal of obtained product values, one receives a parameter that describes the dynamics of changes of the charge transfer reaction equivalent to the dynamics of changes of AISI 304 stainless steel dissolution process in conditions of proceeding intergranular corrosion.

Accordingly, Fig. 7 presents dynamic changes of the reciprocal of $R_{ct}{\cdot}C_{dl}$ product vs. reactivation potential determined based on DEIS measurements. It can be observed that the non-sensitized specimen shows slight decrease in the dynamics of changes of the charge transfer reaction with reactivation potential. Decrease by about three orders of magnitude in the dynamics of changes of the charge transfer reaction with reactivation potential can be observed for the sensitized specimens independently of the sensitization time as a result of proceeding cathodic polarization of the examined system. Nevertheless, the dynamics of changes of the charge transfer reaction is very high [$\log(\tau_{ct}^{-1}) \geq 10^2$ s^{-1}], which indicates significant AISI 304 stainless steel dissolution process in the reactivation potential region.

The same procedure was employed in calculating the remaining electrical parameters connected with the intermediate adsorption process, that is L and R_{ads}. Obtained values of $R_{ads}{\cdot}L$ product represent time-constant of the intermediate adsorption process; thus, the converse of these values is directly related to the dynamics of changes of the intermediate adsorption process.

Figure 8 represents the dynamics of changes of the intermediate adsorption process as a function of reactivation potential for the sensitized specimens only. Independently of the sensitization time, the dynamics of changes of the intermediate $(FeOH)_{ads}$ adsorption process decreases from $\log(\tau_{ads}^{-1})=2.3$ to $\log(\tau_{ads}^{-1})=0$ within the reactivation potential range $E=-0.625/-0.750$ V, and finally, below −0.750 V, takes a constant value.

Generally, the dynamics of changes of the intermediate $(FeOH)_{ads}$ adsorption process is lower than the dynamics of changes of the charge transfer reaction. Accordingly, when taking into consideration Figs. 7 and 8 as well as the theory proposed by Armstrong et al. [44] and Epelboin et al. [45] represented by Eqs. 2 and 3, it can be stated that the adsorption reaction controls overall dynamics of changes of the AISI 304 stainless steel dissolution process during proceeding intergranular corrosion.

Light microscope surface micrographs of the examined AISI 304 stainless steel specimens are presented in Figs. 9a–c. The reference specimen did not exhibit any changes in the microstructure under investigated conditions (Fig. 9a). On the contrary, the specimens subjected to sensitization for 24 and 36 h exhibited distinct corrosion failure along grain boundaries (Figs. 9b,c).

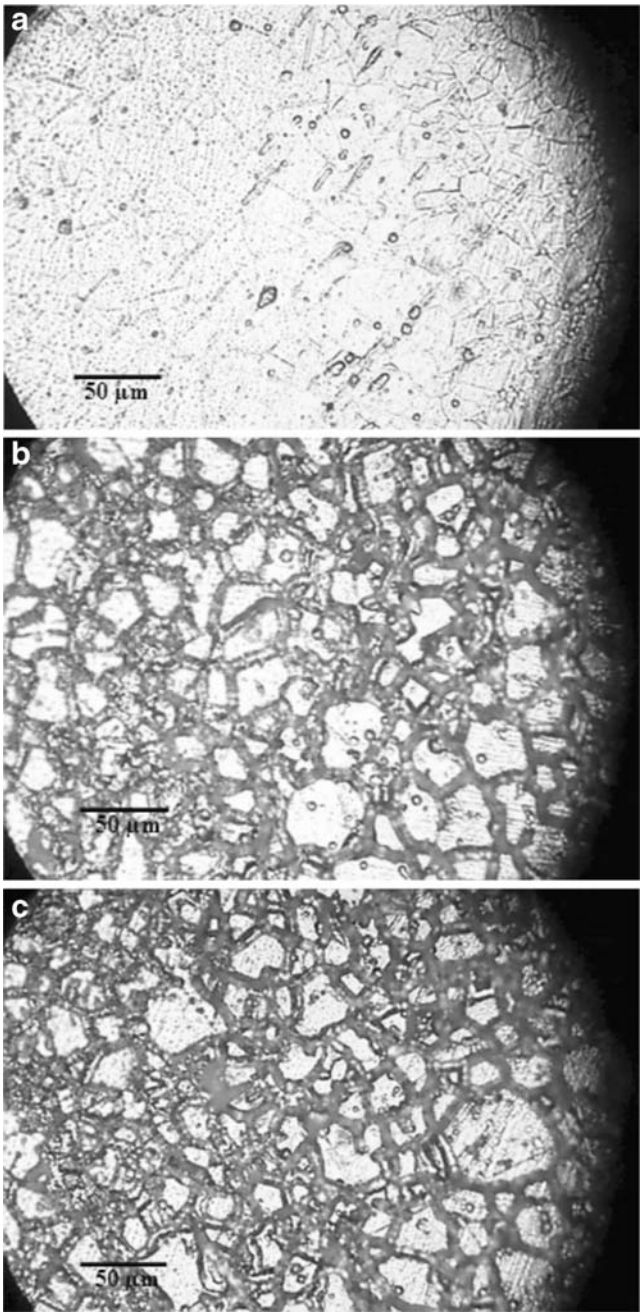

Fig. 9 Light microscope surface micrographs of AISI 304 stainless steel after electrochemical etching in 60% H_2SO_4+0.5 g hexamine solution for 2 min: **a** reference (non-sensitized) specimen, **b** specimen after 24 h of sensitization in 675 °C, **c** specimen after 36 h of sensitization in 675 °C

Conclusions

On the basis of performed research, it can be stated that, with the use of DEIS technique, it is possible to measure dynamic changes of impedance during AISI 304 stainless steel dissolution process, which occurs in conditions of intergranular corrosion. Results presented in this paper demonstrate instantaneous impedance changes of AISI 304

stainless steel dissolution process proceeding during intergranular corrosion that were recorded vs. reactivation potential.

Moreover, the procedure based on the theory of pure iron dissolution in sulfuric acid medium proposed in this paper can be used to assess the rate of intergranular corrosion of AISI 304 stainless steel independently of the parameter of attacked grain boundaries area.

Simultaneously, on the basis of the DEIS measurements, information about the degree of sensitization of the examined material can be obtained. Accordingly, performed research revealed the advantages of the DEIS technique over the classical double-loop electrochemical potentiokinetic reactivation tests when investigating intergranular corrosion process.

Acknowledgments This work has been supported by grant no. N N507 452734 financed by Polish Ministry of Science and Higher Education.

References

1. Lopez N, Cid M, Puiggali M, Azkarate I, Pelayo A (1997) Mater Sci Eng A 229:123. doi:10.1016/S0921-5093(97)00008-7
2. Moura V, Kina AY, Tavares SSM, Lima LD, Mainier FB (2008) J Mater Sci 43:536. doi:10.1007/s10853-007-1785-5
3. Yang S, Wang ZJ, Kokawa H, Sato YS (2007) J Mater Sci 42:847. doi:10.1007/s10853-006-0063-2
4. Sahlaoui H, Makhlouf K, Sidhom H, Philibert J (2004) Mater Sci Eng A 372:98. doi:10.1016/j.msea.2003.12.017
5. Aydogdu GH, Aydinol MK (2006) Corros Sci 48:3565. doi:10.1016/j.corsci.2006.01.003
6. Kelly WK, Rajan RN, Pickering HW (1993) J Electrochem Soc 140:3134. doi:10.1149/1.2220998
7. Gaudet MA, Scully JR (1993) J Electrochem Soc 140:3425. doi:10.1149/1.2221106
8. Bruemmer SM, Arey BW, Charlot LA (1992) Corrosion 48:42
9. Huang CA, Chang YZ, Chen SC (2004) Corros Sci 46:1501. doi:10.1016/j.corsci.2003.09.020
10. Singh R, Chowdhury SG, Kumar BR et al (2007) Scr Mater 57:185. doi:10.1016/j.scriptamat.2007.04.017
11. Michiuchi M, Kokawa H, Wang ZJ et al (2006) Acta Mater 54:5179. doi:10.1016/j.actamat.2006.06.030
12. Kokawa H (2005) J Mater Sci 40:927. doi:10.1007/s10853-005-6511-6
13. Wasnik DN, Kain V, Samajdar I et al (2004) Mater Sci Forum 467–470:813
14. García C, Martín F, de Tiedra P, Blanco Y, Ruíz-Roman JM, Aparicio M (2008) Corros Sci 50:687. doi:10.1016/j.corsci.2007.10.001
15. Sidhom H, Amadou T, Sahlaoui H, Braham C (2007) Metall Mater Trans A 38:1269. doi:10.1007/s11661-007-9114-9
16. France WD, Greene ND (1968) Corrosion 24:403
17. Payer JH, Staehle RW (1975) Corrosion 31:30
18. Chung P, Szklarska-Smialowska S (1981) Corrosion 37:39
19. Cihal V, Stefec R (2001) Electrochim Acta 46:3867. doi:10.1016/S0013-4686(01)00674-0
20. Novak P, Stefec R, Franz F (1975) Corrosion 31:344
21. Umemura F, Akashi M, Kawamoto T, Gijutsu B (1980) Corros Eng Jpn 29:163
22. Pardo A, Merino MC, Coy AE et al (2007) Acta Mater 55:2239. doi:10.1016/j.actamat.2006.11.021
23. Prosek T, Novak R, Bystriansky J (2005) Mater Corros 56:312. doi:10.1002/maco.200403839
24. Cihal V, Lasek S, Blachetova M, Kalabisova E, Krhutova Z (2007) Chem Biochem Eng Q 21:47
25. Terada M, Saiki M, Costa I, Padilha AF (2006) J Nucl Mater 358:40. doi:10.1016/j.jnucmat.2006.06.010
26. Darowicki K, Lentka G, Orlikowski J (2000) J Electroanal Chem 486:106. doi:10.1016/S0022-0728(00)00111-X
27. Darowicki K, Slepski P (2003) J Electroanal Chem 547:1. doi:10.1016/S0022-0728(03)00154-2
28. Darowicki K, Slepski P (2002) J Electroanal Chem 533:25. doi:10.1016/S0022-0728(02)01085-9
29. Park SM, Yoo JS, Chang BY, Ahn ES (2006) Pure Appl Chem 78:1069. doi:10.1351/pac200678051069
30. Darowicki K, Orlikowski J, Arutunow A (2004) Corros Sci Eng Tech 39:255. doi:10.1179/147842204X2844
31. Darowicki K, Krakowiak S, Slepski P (2004) Electrochem Commun 6:860. doi:10.1016/j.elecom.2004.06.010
32. Darowicki K, Krakowiak S, Slepski P (2004) Electrochim Acta 49:2909. doi:10.1016/j.electacta.2004.01.070
33. Darowicki K, Krakowiak S, Slepski P (2005) Electrochim Acta 50:2699. doi:10.1016/j.electacta.2004.11.015
34. Darowicki K, Slepski P, Szociński M (2005) Prog Org Coat 52:306. doi:10.1016/j.porgcoat.2004.06.007
35. Darowicki K, Orlikowski J, Arutunow A (2003) Electrochim Acta 48:4189. doi:10.1016/S0013-4686(03)00604-2
36. Darowicki K, Orlikowski J, Arutunow A (2005) J Electroanal Chem 576:277. doi:10.1016/j.jelechem.2004.10.025
37. Darowicki K, Orlikowski J, Arutunow A, Jurczak W (2005) Electrochem Solid-State Lett 8:B55. doi:10.1149/1.2030468
38. Darowicki K, Orlikowski J, Arutunow A, Jurczak W (2006) Electrochim Acta 51:6091. doi:10.1016/j.electacta.2005.12.054
39. Darowicki K, Orlikowski J, Arutunow A, Jurczak W (2007) J Electrochem Soc 154:C74. doi:10.1149/1.2398880
40. Li LF, Caenen P, Celis JP (2005) J Electrochem Soc 152:B352. doi:10.1149/1.1990127
41. ASTM G108-94 (2001) Standard test method for electrochemical reactivation (EPR) for detecting sensitisation of AISI type 304 and 304L stainless steel. In: Annual Book of ASTM Standards Section 3: Metals Test Methods and Analytical Procedures, Vol. 03.02: Wear and Erosion; Metal Corrosion
42. Gabrielli C (1984) Identification of electrochemical processes by frequency response analysis. Technical Report No. 004/83, 2nd edn., Farenborough
43. Epelboin I, Gabrielli C, Keddam M, Takenouti H (1981) In: Bockris JO'M, Conway BE, Yeager E, White RE (eds) Comprehensive treatise of electrochemistry, vol. 4. Electrochemical Materials Science, New York
44. Armstrong RD, Firman RE, Thirsk HR (1973) Faraday Discuss 56:244. doi:10.1039/dc9735600244
45. Epelboin I, Keddam M, Lestrade JC (1973) Faraday Discuss 56:264. doi:10.1039/dc9735600264
46. The Electrified Interface (2000) In: Bockris JO'M, Reddy AKN, Gamboa-Aldeco M (eds) Modern electrochemistry 2A: fundamentals of electronics, 2nd edn. Kluwer , New York